

Vibrational spectroscopy of semiheavy water (HDO) as a probe of solute hydration*

Maciej Śmiechowski[‡] and Janusz Stangret

Department of Physical Chemistry, Chemical Faculty, Gdańsk University of Technology, Narutowicza 11/12, 80-233 Gdańsk, Poland

Abstract: Vibrational spectroscopy is an ideally suited tool for the study of solute hydration. Nevertheless, water is commonly considered by spectroscopists a difficult solvent to work with. However, by using the isotopic dilution technique, in which a small amount of D₂O is introduced into H₂O or vice versa with formation of semiheavy water (HDO), many technical and interpretative problems connected with measurement of infrared spectra of water may be circumvented. Particularly, the isotopic decoupling of stretching vibrational modes greatly simplifies interpretation of the spectra. Systematic studies conducted in several laboratories since the 1980s up to the present day have provided a vast amount of data, concerning mainly ionic hydration. Many of these experiments have been performed in our laboratory. The analysis method we applied is based on the quantitative version of the difference spectra technique and allows separation of the spectrum of solute-affected HDO from the bulk solvent. This review illustrates the development of vibrational spectroscopy of HDO and spectral analysis methods over the years, as well as summarizes the results obtained for ionic and nonionic solutes, including some general hydration models formulated on their basis.

Keywords: aqueous solutions; difference spectra method; semiheavy water (HDO); hydration; vibrational spectroscopy.

INTRODUCTION

For many years, water and aqueous solutions have been the central subject of solution chemistry. The importance of water is well illustrated by the sheer number of monographs devoted exclusively to it and appearing throughout the recent decades [1–6]. Exceptional properties of liquid water, crucially important for the biochemistry of life, can be unequivocally attributed to extensive hydrogen bonding. A single water molecule can donate two hydrogen bonds (H-bonds) and at the same time accept a further two. This property, unusual for such a small molecule, determines the observed “peculiarities” of liquid water as compared to other molecular liquids. Furthermore, H-bonds in water are cooperative, i.e., the energy of water interaction with H-bond donor and acceptor is non-additive. The interaction with donor depends largely on the polarizing power of the acceptor and vice versa. The phenomenon of cooperativity is a key to proper interpretation of the properties of solutions, manifested by many of their observable attributes, including vibrational spectra. This was first noted in the classic work of Frank and Wen [7], although the practical application in vibrational spectra interpretation had to wait for its advent for the next three decades [8,9].

*Paper based on a presentation at the 31st International Conference on Solution Chemistry (ICSC-31), 21–25 August 2009, Innsbruck, Austria. Other presentations are published in this issue, pp. 1855–1973.

[‡]Corresponding author

Numerous experimental techniques, as well as theoretical simulations, have been applied to study the structure of water and aqueous solutions. The most “direct” results seem to be provided by diffraction experiments, either with X-rays or neutrons [10–13]. However, the necessity to use large solute concentrations and the inherent difficulties in interpretation of data still limit their applicability to some extent. A different and increasingly important branch of water structure studies stems from computational chemistry. Molecular dynamics simulations, pioneered for water by Rahman and Stillinger [14], offer support for experimental data interpretation at a molecular level [10–12]. Their applicability and reliability increase over the years, as available computational power grows. Ultimately, this progress led to the introduction of quantum mechanics to the classical molecular dynamics realm, opening further possibilities for formulation of models explaining experiments [15].

The understanding of ionic hydration phenomena is still a challenging problem for solution chemistry [4,5,16,17]. Several intuitive models of ionic hydrations have been proposed over the years. The one suggested by Frank and Wen has been especially well acclaimed [7]. Their picture of consecutive hydration spheres around a specific ion has proven essentially correct and still provides conceptual guidelines for interpreting experimental results. Although diffraction methods have thus far given a plethora of data on the structure of electrolyte solutions [10,11], the focus is usually on solute–water coordination, rather than the structural and energetic state of the hydrating water molecules themselves. Computational studies usually follow the same approach [15]. The molecular picture of the hydrating water in the vicinity of the ion is, however, equally interesting in revealing the nature of the hydration process. In addition, the more intricate cases of, e.g., amphiphilic ions [18] or so-called “water” ions (H^+_{aq} and OH^-_{aq}) [19], still carry some degree of ambiguity.

Contrary to simpler ionic solutions, the investigations of specific properties of water in biological systems encounter inevitable difficulties: first, because of the high stage of complication of such systems, and second, because of the difficulty in isolating the contribution of water molecules, which are affected by a solute. Therefore, it is often more suitable to study simple model compounds, presenting an isolated type of functional group encountered in biological systems. The constituents of biomolecules often experience a mixed type of hydration, i.e., the hydrophobic hydration of the alkyl chains combined with the electro-/hydrophilic hydration of the charged groups or the electron pair donor/acceptor atoms. The cooperative effects of both types of hydration determine the overall interaction of the molecule with the surrounding aqueous medium [20]. The “iceberg formation” hypothesis formulated by Frank and Evans [21] for a long time dominated the general view of hydrophobic hydration. This description is, however, deceptively simple and was actually termed “misleading” [22], as there is no evidence from various experimental techniques that an ordering of water structure in the vicinity of a hydrophobic particle really takes place [22,23]. Despite these important findings, the sheer complexity of biomacromolecules causes difficulties in elucidating the real nature of their hydration, which has crucial importance for the chemistry of living cells [6,24].

SEMIHEAVY WATER (HDO) VIBRATIONAL SPECTROSCOPY: A HISTORICAL PERSPECTIVE

Vibrational spectroscopy is an ideally suited method for investigation of solute hydration [4,25,26]. The time scale of the response of vibrational spectroscopy, $\sim 10^{-14}$ s in the range of water stretching vibrations, allows registering even relatively short-lived species formed by water molecules influenced by a solute. On the other hand, vibrational spectrum of liquid water is difficult to register and presents some fundamental interpretative problems. Due to very high molar absorption coefficient, saturation effects dominate in the stretching vibration region of the transmission spectrum, unless a very thin layer of the liquid is used (less than ca. 3 μm). Maintaining reproducible experimental conditions under such requirements is an uneasy task. The collective nature of the water intramolecular vibrations in the liquid phase adds to the complexity of this task, as the intra- and intermolecular couplings between vibrational modes broaden the absorption spectrum and effectively probe collective motions instead of normal

modes [27,28]. The decomposition of the stretching vibration band of water into physically meaningful components related to different structural states of water molecules is possible and their interpretation is now well understood [29]. However, the influence of the solute on water structure is not easily explained, especially taking into account that the comparison of component band parameters between pure water and solute-affected water requires careful data treatment [30].

Attenuated total reflectance (ATR) spectroscopy provides one valuable alternative to transmittance methods, especially for highly absorbing samples, or those that cannot be studied in transmission mode [31]. It is also generally considered to be the best method for measurement of the mid-infrared spectrum of liquid water [32]. The major drawback of this technique is that electromagnetic radiation reaching the detector carries information both about the transmission spectrum, probed by the evanescent wave entering the sample, and about the specular reflectance spectrum, due to reflecting the beam from the crystal-sample interface. These and other spectral effects are collectively known as anomalous dispersion [33], and their removal from raw ATR spectra requires a procedure that is not straightforward [34]. Moreover, the ATR spectra of liquid water are subject to the same interpretative difficulties as transmission spectra [29].

The introduction of D₂O into H₂O or vice versa results in the isotopic exchange reaction leading to the production of semiheavy water, HDO.



The above reaction is not quantitative, since its equilibrium constant is ca. 4 (the most recent NMR estimation gave the value 3.86 [35]). Accordingly, in the equimolar D₂O/H₂O mixture the proportion of H₂O:HDO:D₂O is approximately 1:2:1, as confirmed on the basis of infrared spectra [36]. However, the yield of HDO might be greatly increased by using the isotopic dilution technique. If only a small fraction of D₂O is added to H₂O (or conversely), reaction 1 proceeds to give an almost quantitative amount of HDO [37]. It was checked experimentally that at molar fraction of HDO up to 0.1 the infrared spectral features of HDO seem to be unchanged by the increasing D content [38], suggesting that equilibrium 1 might be considered almost totally right-shifted in these conditions.

There are a number of far-reaching consequences of application of isotopically diluted HDO in vibrational spectroscopic studies. At the molecular level, isotopic substitution effectively decouples the single OD (or OH) oscillator from the surrounding bath [39–41]. The weak intramolecular coupling between OD and OH oscillators within the HDO molecule is unaffected, however, but its magnitude is anyway very small [37]. Some Raman investigations suggest that a very weak coupling due to the presence of D₂O still persists even at D₂O concentrations less than 5 % molar. However, they were based on extrapolation to infinite dilution of D₂O, with the data contaminated with considerable error [41]. Another advantage of isotopic dilution technique is the energetic separation of fundamental modes of HDO, as well as their overtones. Contrary to liquid H₂O or D₂O spectra, the vibrational spectrum of HDO contains sharp, well-defined bands, free of the Fermi resonance-type interactions with overtones [40]. The final benefit from HDO spectra is of a technical nature, namely, the absorption intensity of the diluted HDO molecules in the OD or OH stretching range permits measurements in transmission mode in cells with 30–50 μm path length, much more convenient than ultra-thin films needed for H₂O or D₂O or special equipment needed for high-quality ATR spectra [40].

The question of isotopic fractionation in the hydration sphere with respect to bulk solvent is important for the validity of the results obtained using isotopically diluted HDO as a probe. In general, a non-statistical distribution of the OH and OD oscillators in the hydration sphere might be suspected. The extensive experimental tests for mono- and divalent cations with the infrared spectra of HDO in H₂O and D₂O revealed a very weak effect for divalent cations only, and a possibility of compensation of anionic and cationic effects was suggested [42]. Only for very strongly coordinating trivalent cations (such as Al³⁺) a measureable fractionation was observed, although its exact magnitude was not given

[43]. Therefore, the conclusions obtained on the basis of HDO spectra (either in the OD or OH stretching range) seem to be a valid description of the hydration phenomena.

The potential of HDO as a vibrational spectroscopic probe in water studies was realized early on [40,44,45]. The pioneering infrared experiments were soon followed with Raman investigations [37,41,46–49]. Spectra of isotopically diluted HDO were found to prevent some of the experimental and interpretative problems connected with H₂O spectra, as outlined above. It was also apparent from the beginning of such studies that the decoupled OD/OH water oscillators are a very sensitive probe of ionic hydration [44,45].

The interpretation of the OD stretching vibration contour in terms of molecular interactions in liquid water was a subject of long discussion [37,40,50–52]. Specifically, the concurrent views of “mixture” and “continuum” models of liquid water were critically evaluated. Particularly, Raman spectra of HDO, due to the apparent asymmetry of the OD band, encouraged interpretation in terms of the “mixture” model [37,47,51]. The appearance of a clear isosbestic point in the temperature dependence of Raman spectra was used to give various estimations of the proportion of “non-hydrogen-bonded” oscillators [37,47,51]. However, the same assessment based on infrared spectra was indirect and came out with a different value [52]. Therefore, some authors favored the “continuum” description of liquid water instead, with a broad distribution of H-bond strengths and geometries [40,50].

This fundamental difference persisted also in the studies of electrolyte solutions [44,48–50,52]. The strict “continuum” interpretation of infrared spectra of HDO in aqueous NaCl [50] led to a conclusion that the very concept of defined hydration spheres [7] is “arbitrary”. On the other hand, the “mixture” model proponents extended the two-state description of liquid water to aqueous electrolyte solutions, pointing at the salt-induced H-bond breaking, similar to the effect of temperature increase [48,49,51]. Closely related to this explanation is the concept of “structural temperature,” introduced by Bernal and Fowler [53]. In infrared spectroscopic studies, it is based on an assumption that the spectral effect of a solute might be compared, by proper definition of a certain criterion, to the effect of temperature change on the bulk water spectrum. This approach had some limited success in explaining hydration phenomena, although it was more popular in the near-infrared region, where the spectra are more sensitive to weak H-bonds [51,54]. However, it was quickly postulated that such comparison is an oversimplification of the actual hydration mechanism [50].

The early interpretations of aqueous salt solution spectra were mainly centered on the phenomenon of “band splitting” in the HDO spectrum by specific anions [55–57]. Since from the HDO spectroscopy point of view, anions display more prominent structure-breaking properties in water than cations [18,51], their influence on the OD stretching band was readily detectable, especially at the high solute concentrations employed [44,52]. Weak cationic effect was first noted for a series of hydrophobic tetraalkylammonium cations by Hartman [52] and for alkali metal cations vs. Mg²⁺ by Dryjański and Kęcki and by Adams et al. [55,58].

The investigations of nonelectrolyte hydration using HDO were at first scarce in comparison to salt solution studies [8,9,48,54,59]. Since the non-electrolyte influence on the HDO spectrum at low concentrations is usually small and less apparent than in the case of electrolytes [20,60–62], many of these studies rather focused on HDO diluted in large excess of an aprotic solvent [8,9,59], thus having little resemblance to aqueous solution conditions. Nevertheless, these early studies later allowed the construction of a water donicity scale in various solvents of different electron-donating ability [63]. The fundamental differences between ionic and nonionic solutes in the infrared spectra (e.g., much lower hydration numbers and much more important cooperative effects for the latter) were first summarized by Kleeberg [64].

The most meaningful factor in the interpretation of HDO spectra is the band position. According to the empirical Badger–Bauer rule, the position of the water stretching band changes proportionally with the energy of a H-bond [65], thus allowing characterization of the energetic state of water in the vicinity of the solute. The Badger–Bauer rule was tested experimentally [66,67] and theoretically [68] and found essentially valid for liquid water and other protic solvents combined with different proton ac-

ceptors. The energy scale based on the HDO wavenumber shift in H₂O solutions was constructed recently [18], taking into account the van der Waals interactions in liquid water [69] in addition to the H-bonds.

Apart from the band position, the HDO band shape is also informative, providing a measure of water H-bond energy distribution [40]. Due to the existence of empirical curves, linking the oxygen–oxygen intermolecular distance in water (R_{OO}) with the OD stretching wavenumber (ν_{OD}) [70–72], this energy distribution can be transformed to distance distribution, allowing for a structural characterization of water in the hydration sphere, which is very difficult to obtain directly by diffraction methods [73]. Equation 2 involved in the $\alpha(\nu_{OD})$ to $P(R_{OO})$ transformation was first proposed by Wall and Hornig [46].

$$P(R_{OO}) = C\alpha(\nu_{OD}) \frac{d\nu_{OD}}{dR_{OO}} \quad (2)$$

In eq. 2, C is the normalization constant that normalizes the probability distribution to 1, $\alpha(\nu_{OD})$ is the absorbance and the derivative of the $\nu_{OD}(R_{OO})$ correlation is used. Following some early suggestions [73], the final procedure developed for HDO spectra [22] makes use of the correlation curve 3 by Berglund et al. [70].

$$\nu_{OD}/\text{cm}^{-1} = 2727 - \exp[16.01 - 3.73(R_{OO}/\text{\AA})] \quad (3)$$

This approach was questioned by the results of molecular dynamics simulations, pointing out at a considerable dispersion of the $\nu_{OD}(R_{OO})$ relationship due to the distribution of H-bond angles [74]. This was suggested only qualitatively as early as in 1966 [40]. However, very recent theoretical analysis of time-resolved infrared spectra of HDO in D₂O supports the validity of the $\nu_{OD}(R_{OO})$ correlations, at least in thermal equilibrium conditions (like in traditional infrared spectroscopy) [75].

Many of the fundamental works describing the spectral effects of HDO are due to Luck and co-workers [8,9,68,69,76]. Particularly, the detailed characterization of van der Waals interactions in water [69], the proof of the importance of cooperative effects in liquid water [8,9,76], and the introduction of the weighted difference spectra method [8,76] had significant influence on further studies of hydration phenomena.

Afterwards, infrared spectroscopy of HDO was employed primarily by two research groups: Lindgren and co-workers at Uppsala University [38,42,43,73,77–85] and Stangret and co-workers at Gdańsk University of Technology [18,20,22,60–63,86–94]. The efforts of these two academic centers eventually led to the formulation of generalized models of hydration of ionic and nonionic solutes that will be discussed in detail later [18,60,94].

HDO vibrational spectroscopy is currently exploring a new dimension of time. The appearance of equipment allowing generation of sub-picosecond laser pulses allows the measurement of time-resolved ultrafast infrared spectra in liquid water. The pioneering investigations with the pump-to-probe impulse delay of the order of picoseconds [95] were soon upgraded to the femtosecond range [96]. The observation of vibrational dynamics in liquid water opens new fascinating perspectives for hydration studies. The growing area of ultrafast spectroscopy of water is not, however, the subject of this review, and a thorough summary of the technique can be found elsewhere [97].

DIFFERENCE SPECTRA METHOD: PRINCIPLES AND APPLICATIONS

The attempts to isolate the spectral influence of the solute from the spectrum of the bulk, unaffected solvent were undertaken on numerous occasions, although the earliest of the proposed procedures could be treated as qualitative only.

The easiest solution is, of course, to record the spectra vs. a pure solvent background, eventually accounting for the solvent concentration difference [54,98]. This approach leads only to a simple spec-

tral difference, though, which clearly indicates the trends with respect to bulk solvent, but produces unphysical, hard-to-interpret spectra.

Qualitative means to analyze the influence of the solute on the solvent spectrum were proposed later, and the spectra thus obtained could be treated as real solute-affected solvent spectra, not just mere spectral differences. The different procedures used for this purpose were termed variously as “double difference technique” [77], “weighted difference spectra” [8,76], and “differential spectra analysis” [99,100].

The quantitative procedure that allows elimination of the bulk water contribution from the solution spectra in order to obtain the solute-affected water spectrum was proposed in 1988 [38,86]. The two procedures proposed independently by Stangret [86] and by Kristiansson, Lindgren, and de Villepin [38] are known as “difference spectra method” and “double difference technique”, respectively.

The difference spectra method [86], which is outlined in detail below, is based on the normalization of the experimental spectra recorded at varying molality of the solute, first proposed by Mundy and Spedding [99], coupled with the computer band shape analysis introduced by Kristiansson, Eriksson, and Lindgren [77]. Later modifications to the original procedure increased its reliability and considerably simplified the analysis [22]. Although this review concentrates on water as the solvent used, the method is far more general and can be used whenever the spectrum of any component of the system can be divided into spectra of unaffected (“bulk”) and affected component (see, e.g., [101] for an example of a biochemical application to Raman spectra of DNA affected by metal ion complexation).

The standardization of the spectra is based on an approximation of the $\varepsilon(\nu_i)$ values versus molality m within the whole spectral series (a series of spectra of a given system measured at different concentrations of the solute). This approximation is based on a least-squares regression at each wavenumber ν_i , where a linear or quadratic relationship is usually found to fit the data adequately [86,99].

The difference spectra method is based on the assumption that the solvent in solution may be divided into additive contributions of bulk (b) and solute-affected (a) solvent. Accordingly, the total concentration of the solvent in the solution ($c/\text{mol dm}^{-3}$) is a sum of both solvent contributions ($c = c_a + c_b$). Assuming that the absorbance additivity principle is valid in this case, eq. 4 relates the molar absorptivity spectra of the bulk and affected solvent to the experimental spectrum of the solution, $\varepsilon(\nu_i)$.

$$\varepsilon c = \varepsilon_a c_a + \varepsilon_b c_b \quad (4)$$

The bulk solvent spectrum is by definition equal to the pure solvent spectrum. By rearrangement of eq. 4 accounting for additivity of concentrations, the unknown spectrum of the affected solvent might be calculated.

$$\varepsilon_a = \frac{c}{c_a}(\varepsilon - \varepsilon_b) + \varepsilon_b \quad (5)$$

The solvent concentrations from eq. 5 can be expressed using molality of the solution as $c = 1/MV$ and $c_a = Nm/V$, where $M/\text{kg mol}^{-1}$ is the molar mass of the solvent (usually $\text{H}_2\text{O} + 4\% \text{ w/w D}_2\text{O}$), $m/\text{mol kg}^{-1}$ is the molality of the solution, V/dm^3 is the volume of solution containing 1 kg of the solvent and m moles of the solute, and the so-called “affected number” N will be discussed in detail later. The quantity V may be obtained from the experimentally known density ($d/\text{kg dm}^{-3}$) and molality of the solution via eq. 6, where $M_s/\text{kg mol}^{-1}$ is the molar mass of the solute.

$$V = \frac{1 + mM_s}{d} \quad (6)$$

Substituting the above expressions for concentrations into eq. 5 gives the final formula for determination of the solute-affected solvent spectrum:

$$\varepsilon_a = \frac{1}{NM} \frac{(\varepsilon - \varepsilon_b)}{m} + \varepsilon_b \quad (7)$$

The fraction $(\varepsilon - \varepsilon_b)/m$ can be referred to as the difference spectrum, though in reality the spectral difference $\varepsilon - \varepsilon_b$ is additionally scaled by molality of the solution. When $m \rightarrow 0$, eq. 7 reduces to

$$\varepsilon_a = \frac{1}{NM} \left(\frac{\partial \varepsilon}{\partial m} \right)_{m=0} + \varepsilon_b \quad (8)$$

The above-mentioned approximation procedure of $\varepsilon(\nu_i)$ vs. m allows calculation of the respective molar absorptivity derivative at each wavenumber ν_i . Equation 8 makes the basis for extraction of a solute-affected solvent spectrum extrapolated to infinite dilution conditions.

Equations 7 and 8 assume that the affected number N is known. This parameter is equal to the number of moles of solvent affected by one mole of solute. It should not be confused with “hydration number” or “solvation number” (in the sense of the parameter obtained from diffraction experiments or molecular dynamics simulations [10,11]). N is close to the hydration number derived from “direct” methods only when the solute-affected HDO band differs sufficiently from the bulk HDO band, either in position or in half-width. Otherwise, the affected number is usually lower than the hydration number. However, the solute-affected HDO spectrum carries structural and energetic information about a greater number of solvent molecules surrounding the solute molecule, depicting the water status in a somewhat “condensed” form [22]. This, along with the short time scale of vibrational spectroscopy, is the main cause of the high sensitivity of the method to differentiate various states of solvent molecules in the solution.

The proper value of the affected number is found basing on the published algorithm [22]. In brief, the trial solute-affected solvent spectrum for a given N value is fitted using the baseline, analytical bands, and the bulk solvent spectrum. The minimal number of analytical bands, which give an adequate fit, is considered as the right number of component bands. This can be verified by examination of the second derivative of the trial-affected spectrum: the plot of this derivative shows minima that approximately illustrate the positions and the number of underlying component bands [88]. The product of Gaussian and Lorentzian peak functions is used as the starting analytical band shape, but it might be replaced later by a pure function for a given band if the contribution of the other component is found negligible. All parameters (including Gaussian to Lorentzian ratio) are unconstrained during the fit, with the exception of the bulk solvent spectrum, for which only intensity is allowed to vary. The maximum value of N , for which the solute-affected solvent spectrum still contains a negligible amount of the bulk solvent spectrum (the practical threshold value is set at 0.5 % of the total integrated intensity of the ε_a spectrum) is considered as the “true” value of N , and the corresponding ε_a spectrum as the “true” affected solvent spectrum. Thus, both unknowns are obtained simultaneously.

Recently, we have also proposed a different, chemometric method of finding the N value [102], making use of target factor analysis and similarity analysis [103]. This method is still in the testing phase, though, so the preliminary results obtained with it will not be reviewed further in this work.

The obtained affected water spectrum provides invaluable energetic and (indirect) structural information about water in the solute’s hydration sphere only, as the bulk solvent’s influence is quantitatively separated. The analytical component bands in such a spectrum have strict physical significance and correspond to various types of intermolecular interactions in the system studied. The first attempts to separate the spectral effects of cation and anion and thus ascribe the component bands to a particular ion were based on strongly structure-breaking anions (such as perchlorate), where the separation of cation- and anion-affected HDO bands allowed their unequivocal assignment [38,73,77,86,87]. Recently, we have been exploring the possibilities of application of ab initio calculations of small aqueous clusters of the studied solutes for interpretation of the component bands in the affected HDO spectra [62,91–94,104]. This allows more unequivocal assignment not only for the more intricate ionic solutes [91–94], but also for the non-electrolytes, for which different hydrogen-bonding patterns are possible [62,104]. Our results were also in agreement with classical molecular dynamics simulations of aqueous solutions of small molecules, if the method of water geometry analysis applied *post hoc* was

compatible with the definition of the oxygen–oxygen distance probability distribution obtained from the affected HDO spectrum [62,104].

The specific applications of the presented methodology to ionic and nonionic hydration and the models formulated on the basis of numerous experiments performed in the past are summarized below.

HDO SPECTROSCOPY IN REVEALING THE TRENDS IN IONIC HYDRATION

Anion hydration

Figure 1 presents OD band positions in maximum (ν_{OD}°) of HDO affected by anions of different kinds, as collected previously in ref. [18], with later additions [89–94]. The values of ν_{OD}° are correlated with polarizing power (q/r , charge divided by ionic radius) of anions. The general trend of linearity of band position shift with polarizing power is apparent. As can be seen, three groups of anions correlate distinctly: I^- , Br^- , Cl^- , and F^- halogen anions (correlation line 1), PF_6^- , BF_4^- , ClO_4^- , NO_3^- , and SO_4^{2-} anions (correlation line 2), and phosphate anions (correlation line 3). There are a number of outlying cases as well, including the amphiphilic anions CF_3SO_3^- , CF_3COO^- , and $\text{C}_2\text{H}_5\text{SO}_4^-$, the hydrophobic anion Ph_4B^- , and the hydroxide anion OH^- .

In the set of anions shown in Fig. 1, originally only F^- and SO_4^{2-} were thought to interact with water stronger than water with water does (basing on the Badger–Bauer rule) [18]. However, our recent additions to the original model increased this number by four further anions: OH^- , H_2PO_4^- , HPO_4^{2-} , and PO_4^{3-} [92,93]. The remaining anions can be considered as water “structure breakers”, since the validity of the Badger–Bauer rule implies that due to ν_{OD}° for anion-affected HDO being higher than for bulk HDO, also the anion–water interaction must be less favorable than water–water interactions in the bulk phase.

The simplest explanation of the shift of correlation line 2 toward higher wavenumbers, with respect to correlation line 1, is the higher number of lone electron pairs of anions in group 2. This ensures lower partial negative charge on centers of interaction with water [18]. However, both lines run approximately in parallel, meaning that the polarization of water molecules with increasing anion’s polarizing power in both series of anions is approximately the same. On the contrary, the slope of relationship 3 for the phosphate family is less steep than for the other two lines. Extension of correlation line 2 determined by polyatomic anions proves that PO_4^{3-} fits adequately in this group. Thus, PO_4^{3-} is similar to all other tetrahedral oxoanions forming line 2, and the rather significant red shift of the HDO band it causes can be attributed exclusively to its large polarizing power. However, both hydrogen phosphate anions apparently possess more pronounced water structure-making properties than expected from their polarizing power. The points representing both anions in Fig. 1 were based on the HDO bands ascribed to interaction, in which the H-bond is donated from a water molecule to the anion, to facilitate comparison with other anions, for which this type of interactions are solely found. A detailed analysis of H-bonding patterns in the vicinity of the discussed anions led to a tentative explanation that the increased polarization effect is caused by the cooperativity of H-bonds from water to anion and those from anion to water, which effectively strengthens the whole hydration sphere, causing the observed ν_{OD}° red shift with respect to other polyatomic anions [93].

The abscissa determined by the intersection of correlation lines 1 and 2 with ν_{OD}° level of the bulk HDO (2509 cm^{-1}) in Fig. 1 correspond to the anion radii below which water–anion interactions become stronger than water–water interactions. Such “critical radius” for the halogen ions is about 1.6 \AA , while for polyatomic anions it is about 1.37 \AA (assuming a monovalent anion).

Extremely weak interaction with water is exhibited especially by the PF_6^- anion ($\nu_{\text{OD}}^{\circ} = 2666\text{ cm}^{-1}$) and to a lesser extent by the BF_4^- anion ($\nu_{\text{OD}}^{\circ} = 2647\text{ cm}^{-1}$). The ν_{OD}° values are clearly higher than ν_{OD}° for HDO molecules which do not form H-bonds with H_2O in water environment (2644 cm^{-1} [37]). Such a high value of ν_{OD}° can be explained by weaker dispersive forces between water and the fluorine atoms of the discussed ions than those between water molecules. Nonetheless,

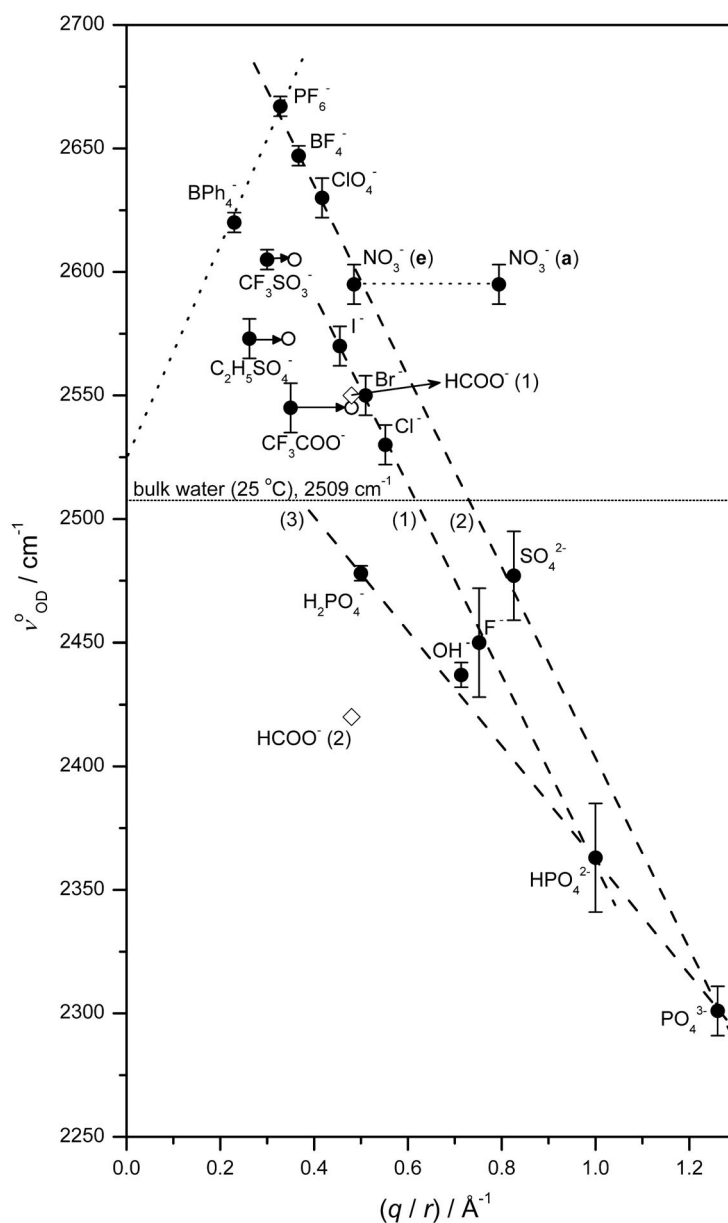


Fig. 1 Relationship between for HDO affected by anions and the polarizing power of anions (q/r): the ν_{OD}° values taken from ref. [18] and references therein, as well as refs. [89–94] (●). q – charge of the anion; $r/\text{\AA}$ – anion radius, based on refs. [4,10,11,16], and refs. therein. For NO_3^- , the ionic radii for equatorial (e) and axial (a) positions have been distinguished [10]. (○) Hypothetical positions for $\text{C}_2\text{H}_5\text{SO}_4^-$, CF_3SO_3^- , and CF_3COO^- without radius contribution of nonpolar groups (as an approximation, r values for HSO_4^- , HSO_3^- , and HCOO^- were used). The dashed line is the expected approximate relationship for hydrophobic anions (see text). For HCOO^- , the positions of two affected HDO bands have been given [94] (see text).

weak anion–water H-bonds exist in both the above cases because monomeric HDO molecules entrapped between $-\text{CF}_3$ groups of amphiphilic anions in a micelle-type cage exhibit a band at $\nu_{\text{OD}}^{\circ} = 2692 \text{ cm}^{-1}$ [18].

The NO_3^- anion is another interesting example in that group of anions. Diffraction data indicate that this planar anion interacts with water more strongly in the axial positions (through the nitrogen atom) than in the equatorial plane (through the oxygen atoms) [10,11]. Points corresponding to each radius of interaction have been shown separately in Fig. 1. From correlation 2, it appears that water affected by the anion corresponds mainly to equatorial interactions, whereas water in the axial positions resembles bulk water (as proven by projecting the point corresponding to axial interactions vertically to an intersection with the correlation line). This visualizes the physical significance of the affected water spectrum, as well as the difference between the number of affected water molecules (N) and the coordination number (in a sense of the number of nearest neighbors).

The behavior of the amphiphilic anions is difficult to rationalize. As can be seen in Fig. 1, ν_{OD}° values for amphiphilic anions lay much below correlation line 2, which seems most suitable for comparison with ions of this type. If the radii of only the hydrophilic part of these anions are considered in the calculation of q/r values, the points are anticipated to shift toward correlation line 2. Because this is not the case, the interaction with water does not seem to depend on the hydrophilic group only. This suggests that nonpolar groups strengthen the water structure weakened in the surrounding of the polar groups [18]. On the basis of the distance between open points (in the vertical direction), representing q/r values of the hydrophilic part, and correlation curve 2, it can be estimated that the CF_3 group and the C_2H_5 group shift the band by about 50 and 75 cm^{-1} , respectively, toward lower wavenumbers. Another important effect that stabilizes the hydrated anion structure stems from cooperativity of the hydrophobic- and electrophilic-type interactions between the anion and water [20]. The carboxylic anions, closely related to the discussed group, are represented in the diagram by a single case of formate [94]. It is seen that neither of the two bands attributed to the anion-affected water fits into the model: the first one closely resembles the CF_3COO^- case, while the second one loosely corresponds to the band position for OH^- . The implications of the two-band spectrum for carboxylate-affected water will be discussed later in the chapter devoted to hydration of nonelectrolytes and biomolecules.

The only example of a purely hydrophobic anion in Fig. 1 is Ph_4B^- . As can be seen, it strongly weakens water H-bonds ($\nu_{\text{OD}}^\circ = 2620 \text{ cm}^{-1}$). The effect is, however, not as strong as can be expected from the large anion radius. This seems to indicate that water molecules surrounding the anion form, to some extent, H-bonds between each other. This may be possible when water molecules tend to be positioned tangentially to the surface of the ion, resulting in sufficiently low orientation energy. The respective band positions for hydrophobic cations, Ph_4P^+ ($\nu_{\text{OD}}^\circ = 2530 \text{ cm}^{-1}$) and Bu_4N^+ ($\nu_{\text{OD}}^\circ = 2523 \text{ cm}^{-1}$) are clearly at much lower wavenumbers as compared with the Ph_4B^- anion ($\nu_{\text{OD}}^\circ = 2620 \text{ cm}^{-1}$). Thus, cations have a weaker orientating power than anions. The dotted line in Fig. 1 indicates the proposed direction of the band position change with respect to the polarizing power of hydrophobic anions, however, the limited number of studied solutes limits its reliability.

The final outlying point in Fig. 1 corresponds to the hydroxide anion ($\nu_{\text{OD}}^\circ = 2437 \text{ cm}^{-1}$). It is isoelectronic with the fluoride anion and has very similar hydration enthalpy and ionic radius [16]. It would then be expected that OH^- should fit into correlation 1. On the contrary, it is seen that an additional red shift of ν_{OD}° by ca. 35 cm^{-1} is induced by OH^- . This anion has a largely asymmetric hydration sphere: it is a good proton acceptor, probably accepting four H-bonds from water at the oxygen site, while at the same time being a very poor proton donor (a very weak band at $\nu_{\text{OD}}^\circ = 2658 \text{ cm}^{-1}$ for OD^-) [92]. Therefore, it is less surprising that its properties are different from the fluoride anion, which possesses an isotropic hydration sphere. The possible influence of high mobility of the hydroxide anion in an aqueous solution on vibrational spectra of HDO is discussed below, together with the hydrated proton case.

Cation hydration

Figure 2 lists ν_{OD}° values for HDO affected by different cations, as collected previously in ref. [18], with later additions [89–91]. The values of ν_{OD}° are correlated with polarizing power (q/r) of the cations. Unlike anions, cations do not change the position of affected water band in a continuous way. The lack of continuity in ν_{OD}° changes for cations was noticed for the first time by Lindgren et al. [78], basing on the relatively limited set of data available at the time. They indicated two levels: ~ 2525 and $\sim 2420 \text{ cm}^{-1}$. A much larger set of data led later to the formulation of the “band” model of cation hydration [18], which was later altered by adding a separate level corresponding to the hydrated proton [91].

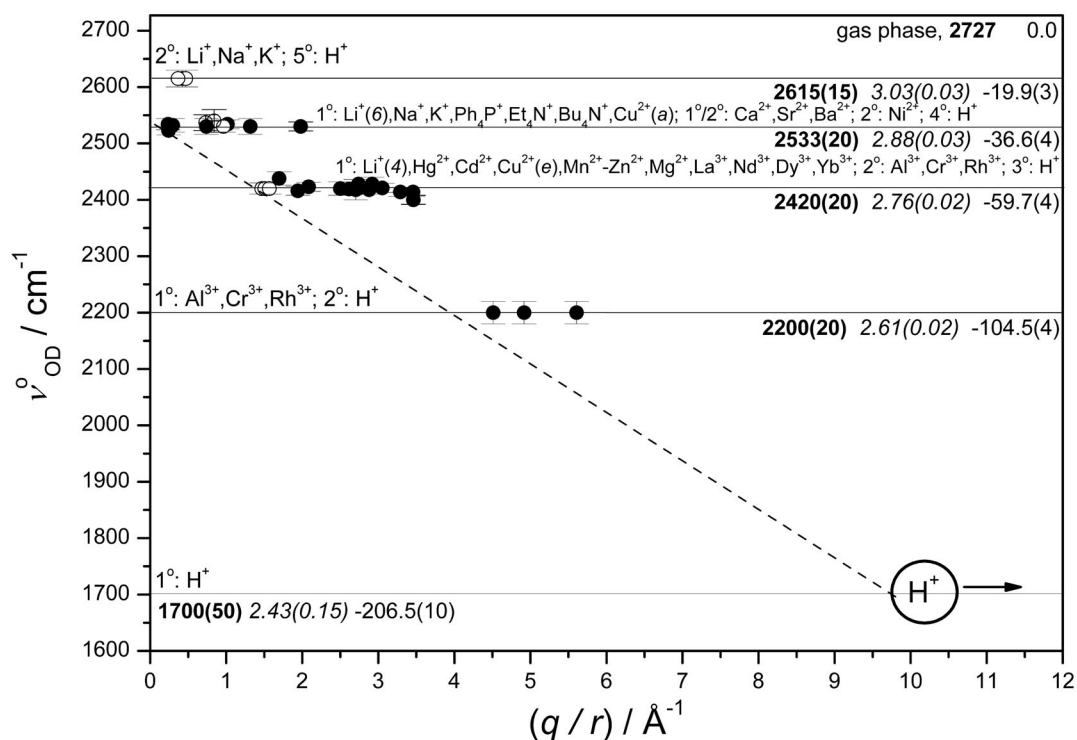


Fig. 2 Relationship between ν_{OD}° for HDO affected by cations and the polarizing power of cations (q/r). ν_{OD}° values taken from ref. [18] and refs. therein, as well as refs. [89–94]. Key: (●) first hydration sphere; (○) second hydration sphere; (⊕) first or second hydration sphere (see text); q – charge of the cations, $r/\text{Å}$ is the cation Pauling radius [10,11,16]. For the second hydration sphere, the effective radius has been calculated as $(r + 1.38 \text{ Å})$, where 1.38 Å is the crystalline radius of water. Cation symbols have been given above the levels; 1°, 2°, etc. refer to the number of hydration sphere. For Cu^{2+} , the points corresponding to axially (a) and equatorially (e) coordinated water are shown [80]; for Li^{+} , the points corresponding to tetra- (4) and hexacoordinated (6) cation are shown [90]. Description of the levels: ν_{OD}° (bold); molar energy of water intermolecular interactions at 25 °C , $\Delta U_{\text{w}}/\text{kJ mol}^{-1}$ (normal); intermolecular oxygen–oxygen distance of water, $R_{\text{OO}}/\text{Å}$ (italic); the scatter of the values (corresponding to the scatter of ν_{OD}° values) is shown in parentheses.

As can be seen from Fig. 2, the ν_{OD}° values for cations arrange themselves in several discrete levels and the corresponding energies of water–water intermolecular interactions appear to be “quantized.” It seems that in aqueous solution a relatively small number of energetic and structural states are preferred. Regularity in the occurrence of these levels may also be observed: the ratio of distances between them amounts to 2.0 ± 0.25 .

The individual energetic and structural states of HDO molecules affected by cations in their first hydration sphere might be characterized as follows, taking into account the $\nu_{\text{OD}}(R_{\text{OO}})$ correlation (3) [70] and the interatomic interaction energy of water (ΔU_{w}) obtained using the Badger–Bauer rule [18]:

The level at $\nu_{\text{OD}}^{\circ} = 1700 \pm 50 \text{ cm}^{-1}$ has the hydrated proton as its sole representative. The isotopically diluted D^+ seems to form a deformed Zundel-type complex ($\text{H}_2\text{O}\cdots\text{D}^+\cdots\text{OH}_2$), and the structural and energetic parameters are in accordance with the unique character of the hydrated proton in an aqueous solution ($\Delta U_{\text{w}} = -206.5 \pm 10 \text{ kJ mol}^{-1}$, $R_{\text{OO}} = 2.43 \pm 0.15 \text{ \AA}$) [91]. The polarizing power of the free proton is impossible to represent on the scale applied for other cations, while using the H_3O^+ ionic radius as an approximation (1.38 \AA [16]) leads to serious deviation from the regularities observed at higher levels of the model from Fig. 2 (viz. the dashed line that marks a lower limit of the polarizing power in each of the successive levels). Therefore, the point representing the hydrated proton in the model serves an illustrative purpose only.

The level at $\nu_{\text{OD}}^{\circ} = 2200 \pm 20 \text{ cm}^{-1}$ represents the highly structurized first hydration shell of trivalent metal cations: Al^{3+} , Cr^{3+} , and Rh^{3+} , in which water molecules experience a severe electrostriction effect and form very strong H-bonds with the second hydration sphere ($\Delta U_{\text{w}} = -104.5 \pm 4 \text{ kJ mol}^{-1}$, $R_{\text{OO}} = 2.61 \pm 0.02 \text{ \AA}$).

The level at $\nu_{\text{OD}}^{\circ} = 2420 \pm 20 \text{ cm}^{-1}$ represents divalent transition-metal cations of the Mn^{2+} - Zn^{2+} series as well as Mg^{2+} , Cd^{2+} , Hg^{2+} , and lanthanides. It also describes the water interactions around Li^+ ion, in the first hydration sphere of the four-coordinated cation [18,90], though some authors did not find the band of HDO affected by Li^+ in this region [78]. This level may be characterized with $\Delta U_{\text{w}} = -59.7 \pm 4 \text{ kJ mol}^{-1}$, $R_{\text{OO}} = 2.76 \pm 0.02 \text{ \AA}$.

The level at $\nu_{\text{OD}}^{\circ} = 2533 \pm 20 \text{ cm}^{-1}$ is the first one, in which the water molecules form (slightly) weaker H-bonds than in pure water ($\Delta U_{\text{w}} = -36.6 \pm 4 \text{ kJ mol}^{-1}$, $R_{\text{OO}} = 2.88 \pm 0.03 \text{ \AA}$). It is occupied by alkali metal cations, alkaline earth metal cations, and hydrophobic cations (Ph_4P^+ , Et_4N^+ , and Bu_4N^+). Several of the cases belonging to that level require further clarification. The lithium cation, already accounted for in the previous level, is represented here by another component band in the affected HDO spectrum [18,90]. On the basis of a rather low affected number for lithium salts, we proposed that it represents the water molecules in the first hydration sphere of the hexacoordinated cation [90], possessing weaker structure-making properties than the tetraordinated form. The diffraction data for Li^+ are highly variable, and equilibrium between 4 and 6 coordination number in aqueous solution seems highly probable [10,11]. For Cu^{2+} , also present in the previous level, the discussed point represents water molecules coordinated axially to the Jahn–Teller distorted hydrated cation, while the energetically more favorable level at 2420 cm^{-1} represents equatorial water molecules [80]. The alkaline earth metal cations (Ca^{2+} , Sr^{2+} , and Ba^{2+}) appear to have “transitional” properties. The high asymmetry of the Ca^{2+} hydration band was confirmed in several studies [78,86]. Consequently, it may be considered that the band of water affected by the discussed cations is actually a superposition of component bands having their maxima at the ν_{OD}° characteristic levels at 2420 and 2533 cm^{-1} . The intensity of the component band corresponding to water in the second hydration sphere is clearly dominating. Because of the method of ionic radius calculation, the water bands affected by Ca^{2+} , Sr^{2+} , and Ba^{2+} have been attributed to the second hydration sphere in Fig. 2. A separate group is formed by Ph_4P^+ , Et_4N^+ , and Bu_4N^+ hydrophobic cations (similar properties were noted by us also for the 2-BuNH_3^+ cation [20]). They have a different shape of the water hydration band from that for other cations, very similar to the bulk HDO spectrum [22,88,89]. These cations reveal the same average energy of surrounding water H-bonds as that for bulk water (measured by the position of the gravity center of the hydration band of HDO). Simultaneously, water in the hydration sphere forms more H-bonds, which are slightly weaker than in the bulk water. Such behavior results from lack of polarization of water molecules by hydrophobic cations [22].

The hitherto discussed cases pertained to the first hydration sphere of the cations. However, whenever affected water in further hydration spheres is spectroscopically distinguishable from bulk water, the component bands attributable to it also fit into the presented model. In each of the discussed cases,

the band position of HDO affected by cation in its second hydration sphere lies one level up (in the direction of higher wavenumbers) from the respective position for the first hydration sphere [18]. It was previously suggested that even further coordination spheres might be detected in this way, but this could not be confirmed with the then available experimental data [90]. However, the recent study of the hydrated proton confirmed the existence of several well-defined hydration spheres around it, spanning the entire range of the model from Fig. 2 [91].

This phenomenon was first noted by Bergström et al. for the trivalent metal cations, when apart from the primary affected HDO band at about 2200 cm^{-1} , another smaller one was detected at ca. 2420 cm^{-1} and ascribed to the HDO molecules in the second hydration sphere [43]. More precisely, the higher wavenumber level describes water molecules' interactions between the second and the third hydration sphere of the trivalent cations. A similar behavior was also noted for the Ni^{2+} cation: an additional band at $\sim 2530\text{ cm}^{-1}$ was first detected by Lindgren and co-workers and ascribed to the anion–water interactions of HDO with OD oscillator pointing away from the SO_4^{2-} anion [43]. It was later proposed that it is more probably attributable to the interactions in the cation's second hydration sphere, in parallel to the trivalent ions [18]. Some of the cases, in which unequivocal HDO band assignment to water affected by cations in their further hydration spheres was possible have been included in Fig. 2.

The highest level in Fig. 2 was originally introduced at 2596 cm^{-1} [18] on the basis of one instance only, namely, the NaF salt [83]. The original interpretation was similar to that presented earlier for the Ni^{2+} cation, with F^- behaving similarly to SO_4^{2-} . Later this band was ascribed to the HDO molecules in the second hydration sphere of Na^+ , following the discussion for Ni^{2+} [18]. However, it was found more frequently for various electrolytes, although it was often superimposed with the stronger anion-affected HDO band. On the basis of our study of PF_6^- alkali metal salts [90], we finally ascribed this band to the molecules in the outermost hydration sphere of the cation, influenced simultaneously by the anion. Figure 3 illustrates the discussed band's positions for several anions and shows an approximately linear relationship between the anion-affected HDO band and the “cation + anion”-affected HDO band. Using this correlation, we were able to predict the $\nu_{\text{OD}}^{\circ}(\text{cation} + \text{anion})$ band position for the hypothetical situation where the anion-affected HDO band is identical to the bulk water band. The intersection of the 2509 cm^{-1} abscissa (the position of bulk HDO band maximum) with the correlation

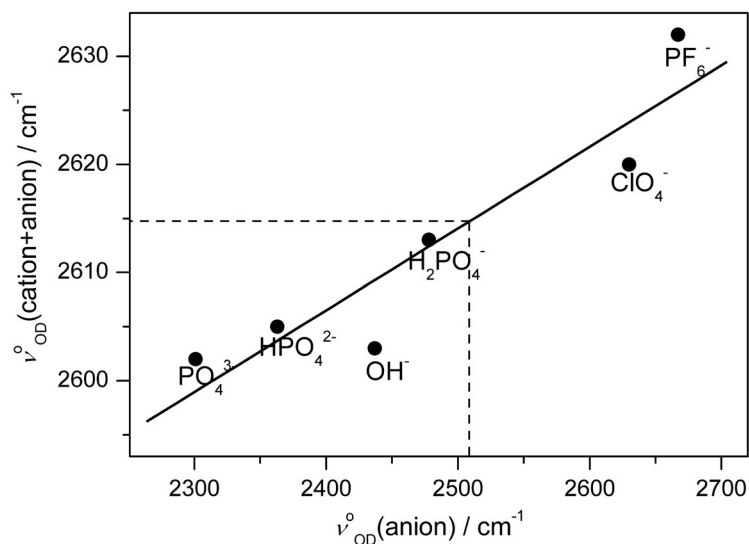


Fig. 3 Dependence of $\nu_{\text{OD}}^{\circ}(\text{cation} + \text{anion})$ on $\nu_{\text{OD}}^{\circ}(\text{anion})$ from experimental data [79,90,92,93] and the predicted linear relationship (solid line). Dashed lines illustrate the point for $\nu_{\text{OD}}^{\circ}(\text{anion}) = \nu_{\text{OD}}^{\circ}(\text{bulk})$ (see text).

line gives an ordinate of ca. 2615 cm^{-1} , which shall be seen as the position of $\nu_{\text{OD}}^{\circ}(\text{cation} + \text{anion})$ band in the absence of an anion and is included as the position of the discussed level in the cation hydration model in Fig. 2. The structural and energetic characteristics ($\Delta U_{\text{w}} = -19.9 \pm 3\text{ kJ mol}^{-1}$, $R_{\text{OO}} = 3.03 \pm 0.03\text{ \AA}$) clearly indicate the existence of a structure-breaking effect of cations in further hydration spheres. This in turn suggests that the model of Frank and Wen [7], with a disordered region encircling the cation's hydration shell, is essentially correct.

NONELECTROLYTE, BIOMOLECULE, AND HYDROPHOBIC HYDRATION STUDIED WITH HDO SPECTROSCOPY

The manner of hydration determines the structure and consequently the activity of macromolecules of biological importance [24]. As already indicated above, for nonionic solutes the mutual influence of nonpolar and electrophilic groups is of key importance [20,60]. For a strictly hydrophobic solute, such as the alkylammonium cations discussed previously in the context of ionic hydration, the population of water H-bonds in their surrounding is higher than for bulk water. That increase is carried on at the expense of weak and so-called “free” OH groups of water. Simultaneously, the average energy of H-bonds does not change considerably because some weakening of H-bonds takes place inside the hydration layer. In other words, water molecules from the hydration sphere of hydrophobic solute form more, but weaker H-bonds, when compared to bulk water. The observed difference consists of different distribution of H-bond energies and corresponding intermolecular distances [22,88,89]. These conclusions are fundamentally different from the “iceberg” hypothesis [21], and it should again be stressed that this term is misleading. No strengthening of H-bonds takes place in the vicinity of the solute, and only an increase of ordering of water is observed. This increase concerns, however, only the average number of H-bonds, as their average energy decreases at the same time. Taking into account the energetic difference between bulk and affected water, it is evident that hydrophobic hydration is a phenomenon of entropic nature [18].

Recently, we have also characterized how hydrophobic effect of the alkyl side chain is influenced by polarizing power exerted on the water molecules by the electrophilic group of 2-butylamine. This effect is cooperatively transmitted to the interactions inside the clathrate-like water “cage” around the alkyl group, effectively strengthening it [20]. The interaction with the donor group does not perturb significantly the already existing hydrophobic “cage” around alkyl chains, consisting of water molecules oriented parallel to the hydrophobic surface. This observation seems to be of general nature and was confirmed for numerous different solutes [60].

To establish quantitatively the correlation between solute properties and HDO spectra, we proposed to use Gutmann donor numbers (DN) [105] as a measure of solute H-bond accepting abilities [60]. The affected HDO band positions characteristic for different solutes were, however, not correlated directly with solvent properties. Firstly, the entire shape of the HDO spectrum should be taken into account to extract as much comparative data as possible. Secondly, the electron-donor solvents are usually characterized by much more asymmetric affected HDO band shape with respect to bulk water. However, when HDO spectra are transformed to intermolecular oxygen–oxygen distance probability distribution function, as described above, the resulting curve is more symmetric for solvent-affected than for bulk HDO. In fact, the distinguishing points of the distribution, namely, its position in maximum (R_{OO}°) and in gravity center (R_{OO}^{c}), are the same, within experimental error, for affected water, whereas bulk HDO is characterized by distinctly separated values (Fig. 4). It is seen that two classes of solvents may be distinguished in Fig. 4: as soon as the solvent's DN rises above the value for monomeric water ($DN = 18$), solutes having stronger electron-donating ability do not change HDO band position considerably and thereby do not change the corresponding intermolecular distances of hydrating water.

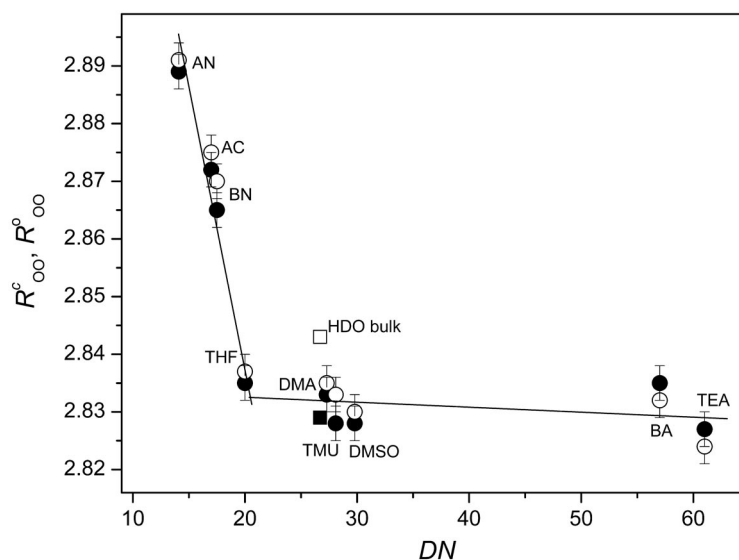


Fig. 4 Correlation of the mean interatomic oxygen–oxygen distance (R^c_{OO} , open circles) and the most probable interatomic oxygen–oxygen distance (R^o_{OO} , full circles) of affected water [60] relative to the donor number [105] of aprotic solvents (AC – acetone, AN – acetonitrile, BA – 2-butylamine, BN – 2-butanone, DMA – dimethylacetamide, DMSO – dimethylsulfoxide, TEA – triethylamine, THF – tetrahydrofuran, TMU – tetramethylurea). The respective distances for bulk water have been shown by square symbols. Errors shown correspond to ± 0.003 Å. Reprinted with permission from *J. Phys. Chem. A* **111**, 1827 (2007). © 2007 American Chemical Society.

Another interesting possibility to compare solute effects on ν^o_{OD} is offered by correlations with solute basicity, expressed as pK_b . The two correlation lines, obtained for anionic solutes and nonelectrolytes, are illustrated in Fig. 5 [94]. The limiting behavior of strong electron donors, already noticed in Fig. 4 with respect to water structure, is also evident here. Apparently, restricted water compressibility prohibits further structure-making properties of electron-donor solutes if their basicity is significantly larger than that of water. However, the presence of electric charge seems to deliver the energy necessary for additional collapse of water structure: the observed shift of ν^o_{OD} to lower wavenumbers by ca. 75 cm^{-1} corresponds to a decrease by about 0.08 Å of the intermolecular oxygen–oxygen distance. Preliminary data for divalent and trivalent anions (those included in Fig. 1) indicate that increasing the charge leads to further tightening of the water structure. Therefore, the term “band model” used for cation hydration [18] is also somewhat applicable to anions. Figure 5 is especially useful in elucidating the mode of carboxylate anions hydration: it is seen that out of the two bands ascribed to anion-affected water (as shown in Fig. 1 on the example of formate) one corresponds to the position of OH^- -affected water, while the second is located approximately at the position of ketone-affected water. These observations might be explained by assuming that interaction of the solvating water with the carboxylic group of the carboxylate anion forces an asymmetric electron distribution between oxygen atoms of this group, so effectively they behave as $\text{C}=\text{O}$ and $\text{C}-\text{O}^-$ groups [94]. Such water-induced symmetry breaking seems to have important implications for hydration of numerous molecules of biological significance.

The hydration of biomolecules is a complex phenomenon [24], in which the above considerations concerning both nonelectrolytes as well as charged groups are important. A useful model of peptide linkage is provided by *N*-alkyl amides, especially *N*-methylacetamide. In our recent work, we determined the hydrophobicity of formamide and acetamide, and their *N*-methyl and *N,N*-dimethyl derivatives, by comparison of the intermolecular oxygen–oxygen distance probability distribution function for

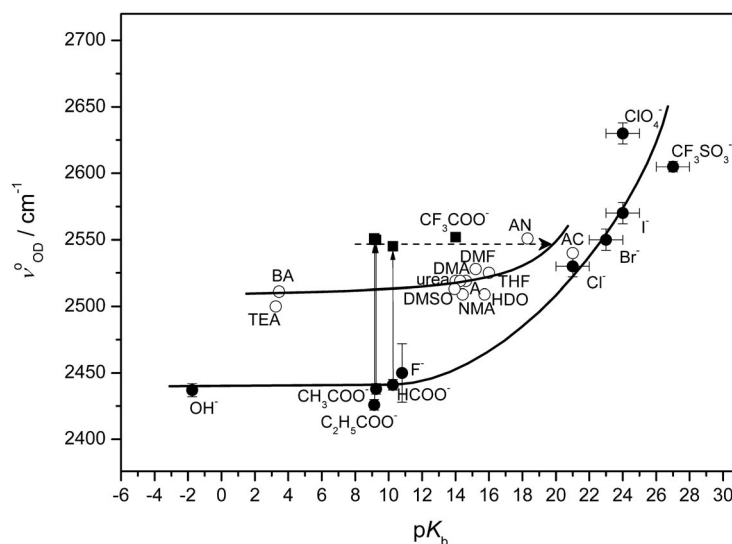


Fig. 5 Correlation of the solute-affected HDO band position in maximum and pK_b value of the solutes [93]. Curves of trend for nonelectrolytes (symbols as in Fig. 4, A – acetamide, NMA – *N*-methylacetamide, DMF – dimethylformamide) and for monovalent anions shown as solid lines, band position of the higher wavenumber component band of carboxylate-affected HDO shown as dashed line, which is at the level of the band position of acetone-affected HDO (see text). Reprinted with permission from *J. Phys. Chem. B* **113**, 7650 (2009). © 2009 American Chemical Society.

the mentioned amides with the model hydrophobic solute (Bu_4N^+) [62]. Apparently, all the amides, with the possible exception of formamide, should be treated as hydrophobic solutes, with *N*-methylacetamide being relatively the most hydrophobic, even though it closely mimics the behavior of the peptide linkage. This means that the stability of native structures of proteins in aqueous solution is controlled mainly by hydrophobic effects. Another interesting aspect closely connected with protein stability in aqueous solution is the influence of osmolytes: small molecules that can display stabilizing or destabilizing activity. The representative compounds for both groups are trimethylamine *N*-oxide (TMAO) and urea, respectively. Recently, we have characterized the hydration of both model compounds using HDO spectroscopy aided by *ab initio* calculations and molecular dynamics simulations [104]. The obtained results show that the H-bonds between the water molecules around TMAO are stronger, shorter, and more linear than those in pure water, forming a clathrate-like network, whereas urea-water H-bonds are very similar to those in pure water. These findings correlate adequately with experiments on water/osmolyte/protein ternary solutions, in which a destabilizing effect of urea was found to be driven mainly by preventing hydrophobic hydration of protein by water. On the other hand, TMAO seems to reinforce the structure of water around protein and thereby promotes hydrophobic hydration [104].

Finally, let us note that even entire biomolecules might be studied as solutes in an aqueous solution with the herein reviewed methodology. Preliminary results obtained by us for lysozyme hydration [106] indicate that a protein molecule is surrounded by water, forming stronger and shorter H-bonds than bulk water, as confirmed by molecular dynamics simulations.

CONCLUSIONS

HDO vibrational spectroscopy is a powerful method in characterizing solute hydration in aqueous solution. The application of the presented difference spectra method leads to the extraction of solute-af-

fect water spectra on the basis of entire solution series. These spectra quantitatively reflect the energetic and structural state of water in the hydration shell of the solute. The obtained results not only reveal the hydration of specific ionic and nonionic solutes, but also enable the formulation of general models of hydration, providing insight into fundamental aspects of this phenomenon. These models reveal, for example, the basic differences between cation and anion hydration, as well as the limiting behavior of the nonelectrolytes' ability to polarize water.

The conclusions reached from infrared HDO spectra have been hitherto supported by numerous experimental and computational techniques, including calorimetry, volumetric measurements, ab initio calculations, and molecular dynamics simulations—in all cases leading to satisfactory agreement between different methods. Therefore, the presented methodology may be seen as soundly based on molecular grounds and able to explain the hydration mode of many new compounds.

ACKNOWLEDGMENTS

We would like to thank all our collaborators from the Department of Physical Chemistry for their contributions to the results reviewed here.

REFERENCES

1. J. L. Kavanau. *Water and Solute-Water Interactions*, Holden-Day, San Francisco (1964).
2. F. Franks (Ed.). *Water: A Comprehensive Treatise*, Vols. 1–7, Plenum Press, New York (1972–1982).
3. W. A. P. Luck (Ed.). *Structure of Water and Aqueous Solutions*, Verlag Chemie, Weinheim (1974).
4. B. E. Conway. *Ionic Hydration in Chemistry and Biophysics*, Elsevier, Amsterdam (1981).
5. H. Kleeberg (Ed.). *Interactions of Water in Ionic and Nonionic Hydrates*, Springer, Berlin (1987).
6. Y. Maréchal. *The Hydrogen Bond and the Water Molecule: The Physics and Chemistry of Water, Aqueous and Bio Media*, Elsevier, Amsterdam (2007).
7. H. S. Frank, W.-Y. Wen. *Discuss. Faraday Soc.* **24**, 133 (1957).
8. H. Kleeberg, G. Heinje, W. A. P. Luck. *J. Phys. Chem.* **90**, 4427 (1986).
9. H. Kleeberg, W. A. P. Luck. *Z. Phys. Chem.* **270**, 613 (1989).
10. Y. Marcus. *Chem. Rev.* **88**, 1475 (1988).
11. H. Ohtaki, T. Radnai. *Chem. Rev.* **93**, 1157 (1993).
12. T. Head-Gordon, G. Hura. *Chem. Rev.* **102**, 2651 (2002).
13. A. K. Soper. *J. Phys.: Condens. Matter* **9**, 2717 (1997).
14. A. Rahman, F. H. Stillinger. *J. Chem. Phys.* **55**, 3336 (1971).
15. B. M. Rode, T. S. Hofer. *Pure Appl. Chem.* **78**, 525 (2006).
16. Y. Marcus. *Ion Solvation*, Wiley Interscience, Chichester (1985).
17. J. Burgess. *Metal Ions in Solution*, Ellis Horwood, Chichester (1978).
18. J. Stangret, T. Gampe. *J. Phys. Chem. A* **106**, 5393 (2002).
19. M. E. Tuckerman, D. Marx, M. L. Klein, M. Parrinello. *Science* **275**, 817 (1997).
20. E. Gojło, M. Śmiechowski, J. Stangret. *J. Mol. Struct.* **744–747**, 809 (2005).
21. H. S. Frank, M. W. Evans. *J. Chem. Phys.* **13**, 507 (1945).
22. J. Stangret, T. Gampe. *J. Phys. Chem. B* **103**, 3778 (1999).
23. J. L. Finney, A. K. Soper. *Chem. Soc. Rev.* **23**, 1 (1994).
24. F. Franks. *Biophys. Chem.* **96**, 117 (2002).
25. W. A. P. Luck. In *Water: A Comprehensive Treatise*, Vol. 2, F. Franks (Ed.), Chap. 4, Plenum Press, New York (1973).
26. R. E. Verrall. In *Water: A Comprehensive Treatise*, Vol. 3, F. Franks (Ed.), Chap. 5, Plenum Press, New York (1973).
27. J. L. Green, A. R. Lacey, M. G. Sceats. *J. Phys. Chem.* **90**, 3958 (1986).

28. D. E. Hare, C. M. Sorensen. *J. Chem. Phys.* **96**, 13 (1991).
29. P. A. Brooksby, W. R. Fawcett. *J. Phys. Chem. A* **104**, 8307 (2000).
30. M. Śmiechowski, J. Stangret. *J. Mol. Struct.* **834–836**, 239 (2007).
31. R. A. Dluhy. *Appl. Spectrosc. Rev.* **35**, 315 (2000).
32. J. E. Bertie, Z. Lan. *Appl. Spectrosc.* **50**, 1047 (1996).
33. R. Belali, J.-M. Vigoureux, J. Morvan. *J. Opt. Soc. Am. B* **12**, 2377 (1995).
34. J.-J. Max, C. Chapados. *Appl. Spectrosc.* **53**, 1045 (1999).
35. J. C. Duplan, L. Mahi, J. L. Brunet. *Chem. Phys. Lett.* **413**, 400 (2005).
36. J.-J. Max, C. Chapados. *J. Chem. Phys.* **116**, 4626 (2002).
37. G. E. Walrafen. In *Water: A Comprehensive Treatise*, Vol. 1, F. Franks (Ed.), Chap. 5, Plenum Press, New York (1972).
38. O. Kristiansson, J. Lindgren, J. de Villepin. *J. Phys. Chem.* **92**, 2680 (1988).
39. A. Sokołowska. *J. Raman Spectrosc.* **22**, 31 (1991).
40. M. Falk, T. A. Ford. *Can. J. Chem.* **44**, 1699 (1966).
41. W. C. Mundy, L. Gutierrez, F. H. Spedding. *J. Chem. Phys.* **59**, 2173 (1973).
42. P.-Å. Bergström, J. Lindgren, O. Kristiansson. *J. Mol. Liq.* **50**, 197 (1991).
43. P.-Å. Bergström, J. Lindgren, M. Read, M. Sandström. *J. Phys. Chem.* **95**, 7650 (1991).
44. R. D. Waldron. *J. Chem. Phys.* **26**, 809 (1957).
45. D. F. Hornig. *J. Chem. Phys.* **40**, 3119 (1964).
46. T. T. Wall, D. F. Hornig. *J. Chem. Phys.* **43**, 2079 (1965).
47. G. E. Walrafen. *J. Chem. Phys.* **48**, 244 (1968).
48. G. E. Walrafen. *J. Chem. Phys.* **52**, 4176 (1970).
49. G. E. Walrafen. *J. Chem. Phys.* **55**, 768 (1971).
50. H. R. Wyss, M. Falk. *Can. J. Chem.* **48**, 607 (1970).
51. W. A. P. Luck. In *Structure of Water and Aqueous Solutions*, W. A. P. Luck (Ed.), p. 221, Verlag Chemie, Weinheim (1974).
52. K. A. Hartman. *J. Phys. Chem.* **70**, 270 (1966).
53. J. D. Bernal, R. H. Fowler. *J. Chem. Phys.* **1**, 515 (1933).
54. J. Paquette, C. Jolicoeur. *J. Solution Chem.* **6**, 403 (1977).
55. P. Dryjański, Z. Kęcki. *Rocz. Chem.* **43**, 1053 (1969).
56. P. Dryjański, Z. Kęcki. *Rocz. Chem.* **44**, 1141 (1970).
57. P. Dryjański, Z. Kęcki. *J. Mol. Struct.* **12**, 219 (1972).
58. D. M. Adams, M. J. Blandamer, M. C. R. Symons, D. Waddington. *Trans. Faraday Soc.* **67**, 611 (1971).
59. D. N. Glew, N. S. Rath. *Can. J. Chem.* **49**, 837 (1971).
60. E. Gojło, T. Gampe, J. Krakowiak, J. Stangret. *J. Phys. Chem. A* **111**, 1827 (2007).
61. J. Stangret, T. Gampe. *J. Mol. Struct.* **734**, 183 (2005).
62. A. Panuszko, E. Gojło, J. Zielkiewicz, M. Śmiechowski, J. Krakowiak, J. Stangret. *J. Phys. Chem. B* **112**, 2483 (2008).
63. J. Stangret. *J. Mol. Struct.* **643**, 29 (2002).
64. H. Kleeberg. In *Interactions of Water in Ionic and Nonionic Hydrates*, H. Kleeberg (Ed.), p. 89, Springer, Berlin (1987).
65. R. M. Badger, S. H. Bauer. *J. Chem. Phys.* **5**, 839 (1937).
66. R. S. Drago, N. O'Bryan, G. C. Vogel. *J. Am. Chem. Soc.* **92**, 3924 (1970).
67. C. N. R. Rao, P. C. Dwivedi, H. Ratajczak, W. J. Orville-Thomas. *J. Chem. Soc., Faraday Trans. 2* **71**, 955 (1975).
68. W. A. P. Luck, T. Wess. *Can. J. Chem.* **69**, 1819 (1991).
69. H. Kleeberg, O. Koçak, W. A. P. Luck. *J. Solution Chem.* **11**, 611 (1982).
70. B. Berglund, J. Lindgren, J. Tegenfeldt. *J. Mol. Struct.* **43**, 169 (1978).
71. A. Novak. *Struct. Bonding* **18**, 177 (1974).

72. W. Mikenda, S. Steinböck. *J. Mol. Struct.* **384**, 159 (1996).
73. O. Kristiansson, A. Eriksson, J. Lindgren. *Acta Chem. Scand.* **38a**, 613 (1984).
74. K. B. Møller, R. Rey, J. T. Hynes. *J. Phys. Chem. A* **108**, 1275 (2004).
75. S. Bratos, J.-C. Leicknam, S. Pommeret. *Chem. Phys.* **359**, 53 (2009).
76. G. Heinje, T. Kammer, H. Kleeberg, W. A. P. Luck. In *Interactions of Water in Ionic and Nonionic Hydrates*, H. Kleeberg (Ed.), p. 39, Springer, Berlin (1987).
77. O. Kristiansson, A. Eriksson, J. Lindgren. *Acta Chem. Scand.* **38a**, 609 (1984).
78. J. Lindgren, O. Kristiansson, C. Paluszkiwicz. In *Interactions of Water in Ionic and Nonionic Hydrates*, H. Kleeberg (Ed.), p. 43, Springer, Berlin (1987).
79. O. Kristiansson, J. Lindgren. *J. Phys. Chem.* **95**, (1991).
80. B. Beagley, A. Eriksson, J. Lindgren, I. Persson, L. G. M. Pettersson, M. Sandström, U. Wahlgren, E. W. White. *J. Phys.: Condens. Matter* **1**, 2395 (1989).
81. P.-Å. Bergström, J. Lindgren. *J. Mol. Struct.* **239**, 103 (1990).
82. P.-Å. Bergström, J. Lindgren. *J. Mol. Struct.* **245**, 221 (1991).
83. P.-Å. Bergström, J. Lindgren, O. Kristiansson. *J. Phys. Chem.* **95**, 8575 (1991).
84. P.-Å. Bergström, J. Lindgren. *Inorg. Chem.* **31**, 1529 (1992).
85. P.-Å. Bergström, J. Lindgren, M. Sandström, Y. Zhou. *Inorg. Chem.* **31**, 150 (1992).
86. J. Stangret. *Spectrosc. Lett.* **21**, 369 (1988).
87. J. Stangret, Z. Libuś. *Spectrosc. Lett.* **21**, 397 (1988).
88. J. Stangret, E. Kamińska-Piotrowicz. *J. Chem. Soc., Faraday Trans.* **93**, 3463 (1997).
89. P. A. Pieniazek, J. Stangret. *Vib. Spectrosc.* **39**, 81 (2005).
90. M. Śmiechowski, E. Gojło, J. Stangret. *J. Phys. Chem. B* **108**, 15938 (2004).
91. M. Śmiechowski, J. Stangret. *J. Chem. Phys.* **125**, 204508 (2006).
92. M. Śmiechowski, J. Stangret. *J. Phys. Chem. A* **111**, 2889 (2007).
93. M. Śmiechowski, E. Gojło, J. Stangret. *J. Phys. Chem. B* **113**, 7650 (2009).
94. E. Gojło, M. Śmiechowski, A. Panuszko, J. Stangret. *J. Phys. Chem. B* **113**, 8128 (2009).
95. R. Laenen, C. Rauscher, A. Laubereau. *Phys. Rev. Lett.* **80**, 2622 (1998).
96. S. Woutersen, H. J. Bakker. *Phys. Rev. Lett.* **83**, 2077 (1999).
97. R. Rey, K. B. Møller, J. T. Hynes. *Chem. Rev.* **104**, 1915 (2004).
98. W. C. McCabe, H. F. Fisher. *Nature* **207**, 1274 (1965).
99. W. C. Mundy, F. H. Spedding. *J. Chem. Phys.* **59**, 2183 (1973).
100. W. C. McCabe, H. F. Fisher. *J. Phys. Chem.* **74**, 2990 (1970).
101. J. Stangret, R. Savoie. *Phys. Chem. Chem. Phys.* **4**, 4770 (2002).
102. P. Bruździak, A. Panuszko, J. Stangret. *Vib. Spectrosc.* (2009). In press. doi:10.1016/j.vibspec.2010.06.006
103. E. R. Malinowski. *Factor Analysis in Chemistry*, John Wiley, New York (2002).
104. A. Panuszko, P. Bruździak, J. Zielkiewicz, D. Wyrzykowski, J. Stangret. *J. Phys. Chem. B* **113**, 14797 (2009).
105. V. Gutmann. *Coord. Chem. Rev.* **18**, 225 (1976).
106. A. Panuszko, P. Bruździak, M. Wojciechowski, J. Stangret. *Book of Abstracts, Xth International Conference on Molecular Spectroscopy*, M. Handke, C. Paluszkiwicz (Eds.), p. 96, P-46, Białka Tatrzańska (2009).